

Intensification of Conductivity and Solubility of Polypyrrole Using Acrylic Acid and Polyacrylic Acid Dopants

P. Meenakshi, M. Selvaraj* and S. Ramu

CSIR-Network Institute of Solar Energy (NISE), CSIR-Central Electrochemical Research Institute, Karaikudi-630006, India

Abstract: Doped polypyrrole (PPy) was synthesized using FeCl_3 as an oxidant, acrylic acid and poly(acrylic acid) as dopants. The effects of dopants and doping level on the solubility and conductivity parameters were optimized. The doped PPy was characterized using FT-IR, UV-Vis and EPR measurements. The thermal stability of doped PPy was studied by TGA/DSC analysis. The morphology of the doped PPy was studied using Scanning Electron Microscope. The Electrochemical study of the doped PPy was carried out by Electrochemical Impedance Spectroscopy (EIS). This study reveals that the polyacrylic acid doped PPy shows higher conductivity than its monomer acrylic acid and the water soluble nature was also augmented at higher doping level of polyacrylic acid on the PPy.

Keywords: Polypyrrole, Acrylic acid, Poly (acrylic acid), EPR spectroscopy, Dopant, Conductivity and EIS studies.

1. INTRODUCTION

Organic conjugated polymers have attracted much attention in recent years for their unique electronic properties. This is due to the π -electron delocalization along the polymer backbone. Due to this property, polypyrrole has a wide range of applications like supercapacitors [1], batteries [2]. The electrical conductivity of the polymers could be increased from the insulating material to the semi conducting material and even to the metallic regime by the doping process with either p-type dopants or n-type dopants. Polypyrrole is one of the most studied conducting polymer due to its easy synthesis and environment stability [3, 4].

These applications are limited to some extent due to low stability towards atmospheric oxidation and lack of processability. As a result the research has been directed towards the preparation of well-defined conjugated polymers with improved processability and stability characteristics. The changes in the electrical conductivity and solubility are influenced not only by the structure and nature of a dopant but also by the doping concentrations and doping procedure [5]. The doped PPy increases the concentration of the charge carrier species in the polymer backbone. The PPy have been doped by many dopants like iodine, HCl, H_2SO_4 , etc to increase the conductivity and solubility. Some of the aromatic acid derivatives and organic sulfonates like dodecylbenzene sulfonic acid (DBSA), p-toluenesulfonic acid (TsOH) are also widely used dopants [6]. Further studies show that adding of large

dopants will reduce the interchain linkage and results in the increase of the conductivity and solubility [7]. Ceren O zdilek etal synthesized the PTSA doped polypyrrole-polytetrahydrofuran graft copolymer [8].

In our study we have synthesized a doped PPy using acrylic acid and poly (acrylic acid) dopants which are low cost materials. Recent studies shows that the PSS (Poly styrene sulfonic acid) doped PPy receives much attention due to its water soluble property. In most cases the doped PPy was insoluble in water except PSS doped PPy. The reaction was carried out at room temperature and also we compared the effect of dopants and dopant concentration at different doping level on the conductivity and solubility properties.

2. EXPERIMENTAL

Pyrrrole (Sigma Aldrich) was purified by distillation under reduced pressure and stored in a refrigerator. The oxidant FeCl_3 (Fischer Chemicals) and the dopants, acrylic acid (Fischer Chemicals), poly(acrylic acid) (Fischer Chemicals) were used as received.

The doped PPy was synthesized using in situ chemical polymerization method. The 0.01 mol purified pyrrole was first dissolved in 50 ml of water with vigorous stirring using magnetic stirrer. The 0.01 mol of dopant (acrylic acid) was dissolved in 25ml of water and added to the pyrrole solution. Oxidant of FeCl_3 was dissolved in 25ml of water and added drop wise to the stirring solution of pyrrole. The reaction was allowed to carried out for 4 hrs at room temperature with stirring. The precipitated PPy was filtered and washed with distilled water. The black PPy was dried in a vacuum oven at 333 K for 8 hrs. The polyacrylic acid doped PPy was also prepared using the same above

*Address correspondence to this author at the CSIR-Central Electrochemical Research Institute, Karaikudi-630006, Tamilnadu, India; Tel: 91-4565-241403; Fax: 91-4565-227779; E-mail: selvaraj58@gmail.com

procedure. The product was washed with the distilled water for several times to remove the polyacrylic acid (water soluble polymer) which was unreacted in the doping process.

In this similar manner, the doped PPy was prepared at different compositions of pyrrole, dopants and oxidants. The composition is given in Table 1.

Table 1: Preparation of AA Doped PPy from Different Ratios of Acrylic Acid and Ferric Chloride Oxidant

Pyrrole (mol)	Acrylic acid (mol)	FeCl ₃ (mol)
0.01	0.01	0.02
0.01	0.02	0.02
0.01	0.03	0.02
0.01	0.04	0.02

Doped PPy products were characterized by FT-IR using Bruker-Tensor 27 model instrument. The UV-Vis spectra of the polymers were recorded using Cary 300 spectrometer. The electron mobility of the doped PPy was recorded by EPR measurements in a Bruker EMX Plus. The thermal stability of the doped PPy was investigated using thermo gravimetric analyzer (SDT Q600 V8.3 Build 101) with nitrogen gas atmosphere. The heating rate was 293 K min⁻¹.

2.1. Electrochemical Impedance Analysis

The Impedance data was recorded in Solarton 2810B using the Nyquist plot as recording software.

The impedance was carried out in a three electrode system at a frequency range of 10 KHz to 0.05Hz. Glassy carbon was used as the working electrode, platinum as the counter electrode and the Ag/AgCl as the reference electrode. The 0.1M of Tetrabutylammonium perchlorate (TBAP) was used as supporting electrolyte. 0.0026g of doped PPy was added to 0.5 ml of the NMP (N-methyl-Pyrrolidone) and finely grinded to make a paste which was coated on the glassy carbon surface (3mm diameter) and dipped into the TBAP solution. Then the impedance was recorded at a particular frequency range.

3. RESULTS AND DISCUSSION

3.1. Vibrational Spectroscopy

The IR spectrum of a pure polypyrrole is shown in Figure 1. The broad and deep peak at 3409 cm⁻¹ is due to the N-H stretching of the pyrrole ring and the peaks at 1552 cm⁻¹ and 1470 cm⁻¹ are due to the typical PPy ring vibrations. The peaks at 1302 and 1043 cm⁻¹ were corresponds to the =C-H bond in- plane vibrations and the broad peak at 1199cm⁻¹ is attributed to N-C stretching vibration. The peak at the 1694cm⁻¹ is owing to the -C=C- stretching vibration of PPy ring. The peaks at 788cm⁻¹ and 925cm⁻¹ indicate the presence of the quinonoid structure of PPy [9]. The peak at 675 cm⁻¹ is due to the C-C out of plane ring deformation [10]. The IR spectrum of acrylic acid doped PPy is shown in Figure 2. The peaks related to PPy were same as discussed above. The peaks at 2900 cm⁻¹ and 2800 cm⁻¹ are due to the C-H stretching vibration of the acrylic acid and the peak in the region of 1631 cm⁻¹ is

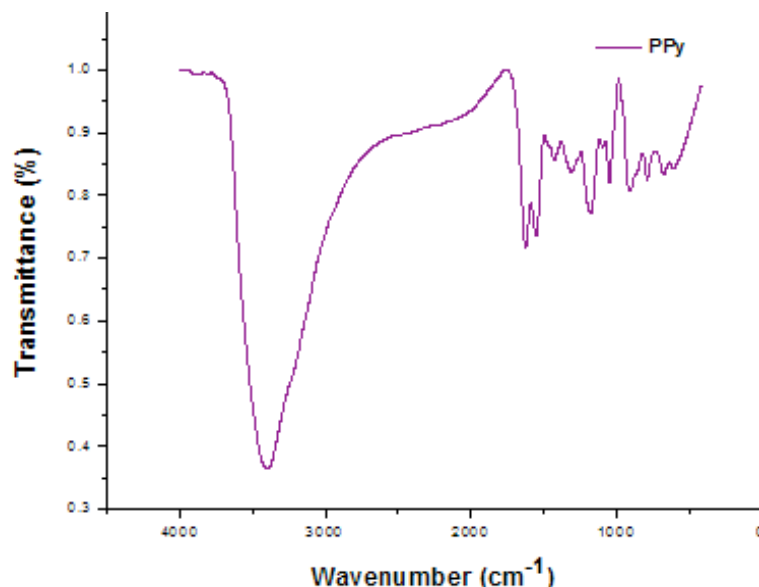


Figure 1: FTIR spectrum of Pure PPy.

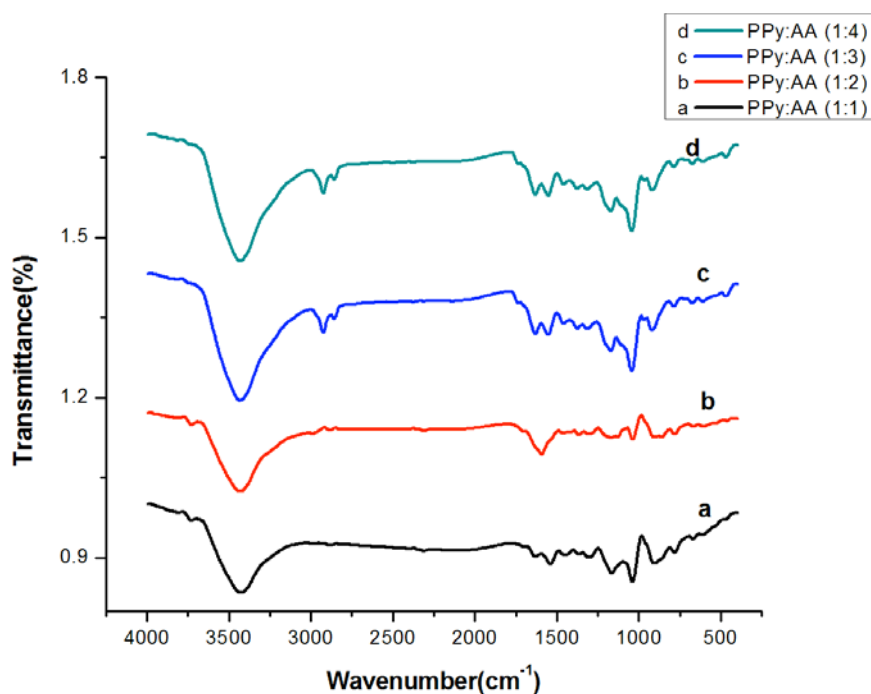


Figure 2: FTIR spectra of acrylic acid doped PPy at different molar ratio of PPy:AA (a) 1 (b) 0.5 (c) 0.33 (d) 0.25.

due to the presence of COO^- stretching vibration of COOH group present in the acrylic acid [11]. The peak at the region of 1410 cm^{-1} is assigned to the $-\text{C}-\text{OH}$ in plane bending stretch which reveals the presence of the free acid group in the polymer matrix [12].

The IR spectrum of polyacrylic acid doped PPy is shown in Figure 3. The peaks at 2900 cm^{-1} is due to the $\text{C}-\text{H}$ stretching vibration of the polyacrylic acid. The band at the region of 1631 cm^{-1} is due to the presence of COO^- stretching vibration of COOH group present in

the polyacrylic acid. The peak at 1700 cm^{-1} is due to the $-\text{C}=\text{O}$ stretching frequency of COOH group. The peak at the region of 1410 cm^{-1} is assigned to the $-\text{C}-\text{OH}$ in plane bending stretch reveals the presence of the free acid in the polymer matrix [12].

3.2. Electronic Spectroscopy

The UV-vis absorption spectrum of pure PPy was shown in Figure 4. This spectrum shows a band at 220 nm and 333 nm . The band at 220 nm is attributed to the

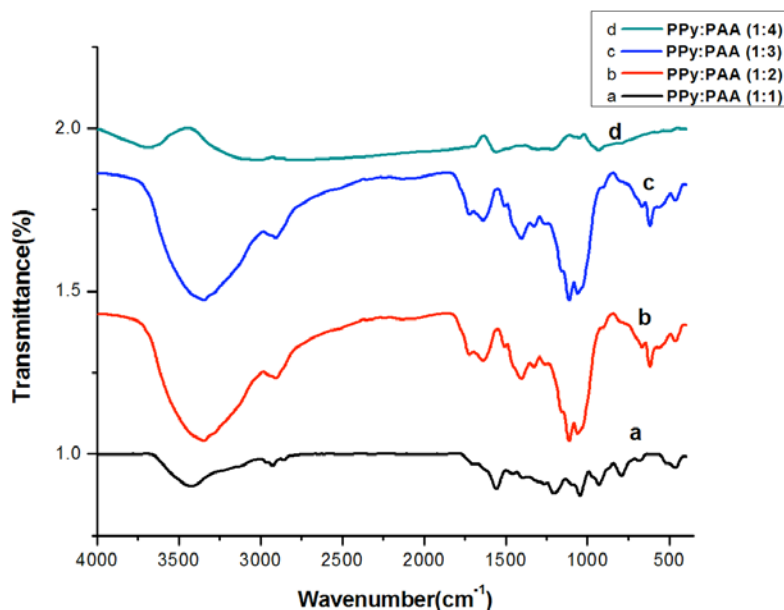


Figure 3: FT-IR spectra of polyacrylic acid doped PPy at different molar ratios of PPy:PAA (a) 1 (b) 0.5 (c) 0.33 (d) 0.25.

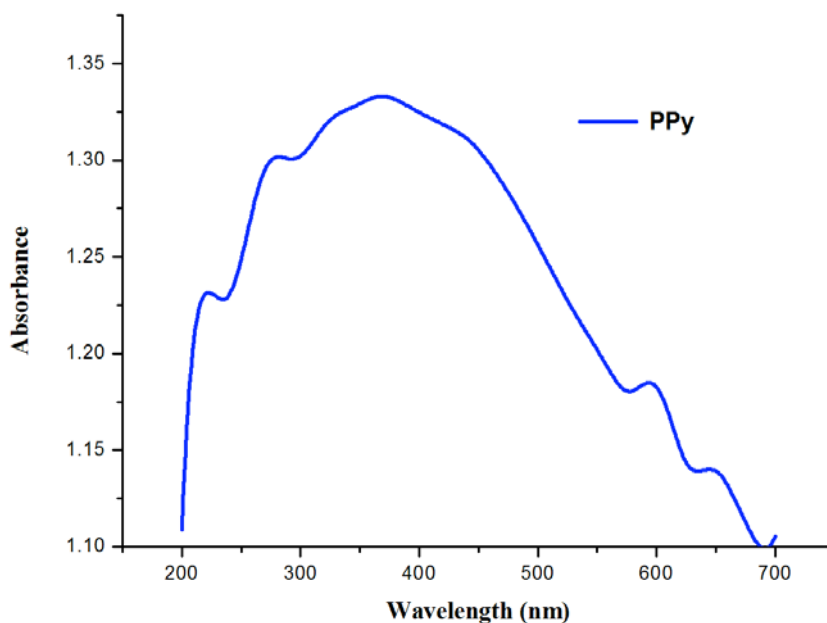


Figure 4: UV-vis absorption spectrum of pure PPy.

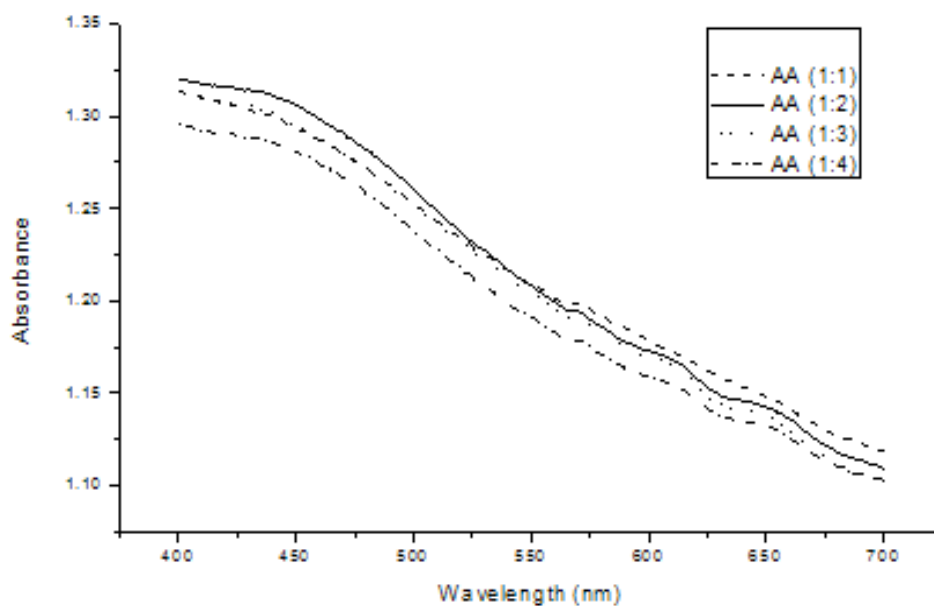


Figure 5: UV-vis absorption spectrum of AA-doped PPy.

π - π^* transition [13] levels which indicates the mobility of lone pair electron in the nitrogen atom of PPy and the transition of free electrons between the quinonoid and benzenoid structure of PPy. The band at 333 nm is due to the n - π^* transition of PPy. Figure 5 shows a band at 600 nm and 650 nm. The band at 600 nm region is due to the presence of polaron band in the doped PPy, which shows that the PPy is in doped state. The band at 650 nm region is due to the presence of bipolaron band. The intensity of the polaron and bipolaron band is low for the 1:1 ratio of doped PPy when compared to other ratios. This shows that the doping level get

increased on increasing the concentration of dopants. Figure 6 shows a band at 220 nm which is due to the presence of π - π^* transition in the PPy ring. The bands corresponding to the polaron and bipolaron was not viewed due to the random delocalization of electrons along the polymer backbone of PAA.

3.3. Electron Paramagnetic Resonance (EPR) Spectroscopy

The EPR spectra of AA and PAA doped PPy was shown in Figures 7 and 8. A single narrow peak in

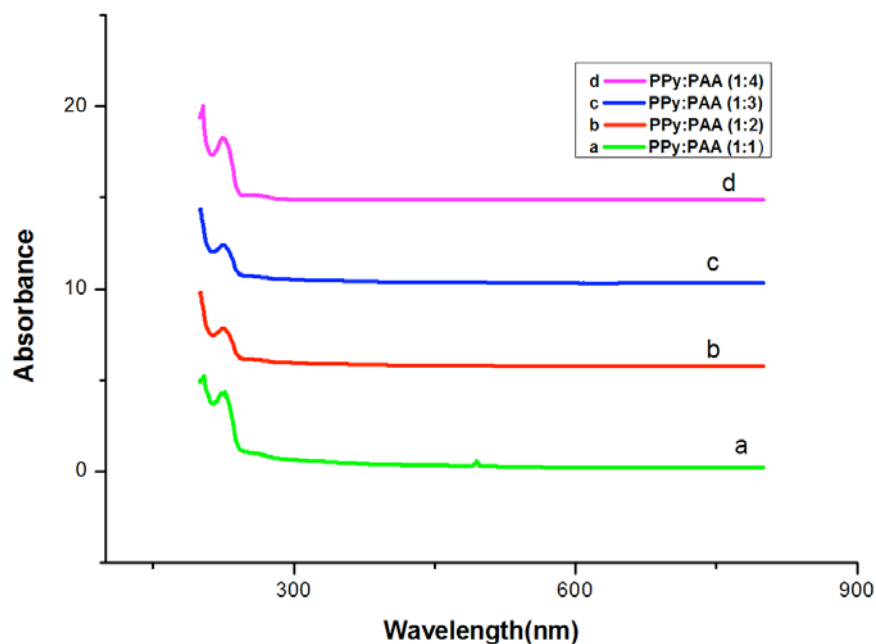


Figure 6: UV-Vis absorption spectra of PAA doped PPy.

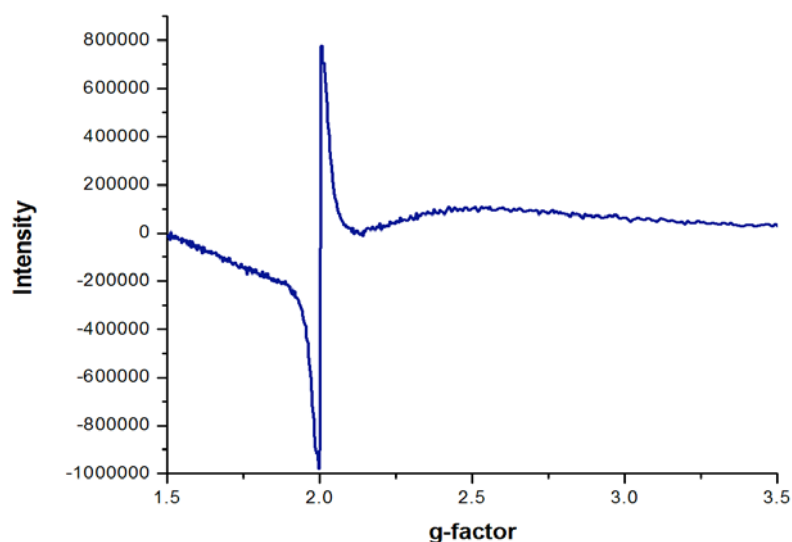


Figure 7: EPR spectra of AA doped PPy.

Figures 7 and 8 confirms the existence of the free electrons in the doped PPy with the 'g' value of 2.0025 and 2.0063 which is in good agreement with the literature value [14]. The width of the EPR signal is directly related to the extent of delocalization of unpaired electrons along the polymer chain. On comparing the Figures 7 and 8, the width of the EPR signal in PAA doped PPy was broader than the AA doped PPy. This shows that the PAA doped PPy (Figure 8) has the large extent of delocalization of unpaired electrons along the polymer backbone than the AA doped PPy (Figure 7). Due to this high delocalization, the PAA doped PPy shows a high conductivity than the AA doped PPy.

3.4. Thermal Studies

The thermal stability of PPy doped with acrylic acid and polyacrylic acid was studied using the TGA and DSC techniques. Figures 9 and 10 show the TGA/DSC graph of acrylic acid and polyacrylic acid doped PPy. Figure 9 shows a curve of weight loss versus temperature for acrylic acid doped PPy. The first significant weight loss at temperature upto 434.03 K [3.9 wt%] was due to the evaporation of the unreacted monomer from the polymer matrix. The second stage weight loss from 524.02 K to 618.41 K [10.28 wt%] was attributed to the degradation of polymer backbone. The third stage weight loss from 618 K was due to the loss

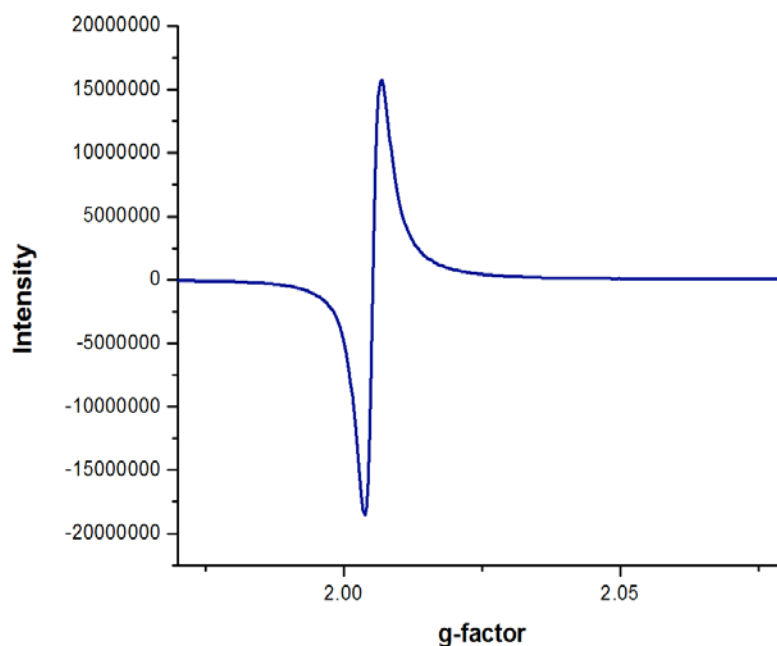


Figure 8: EPR spectra of PAA doped PPy.

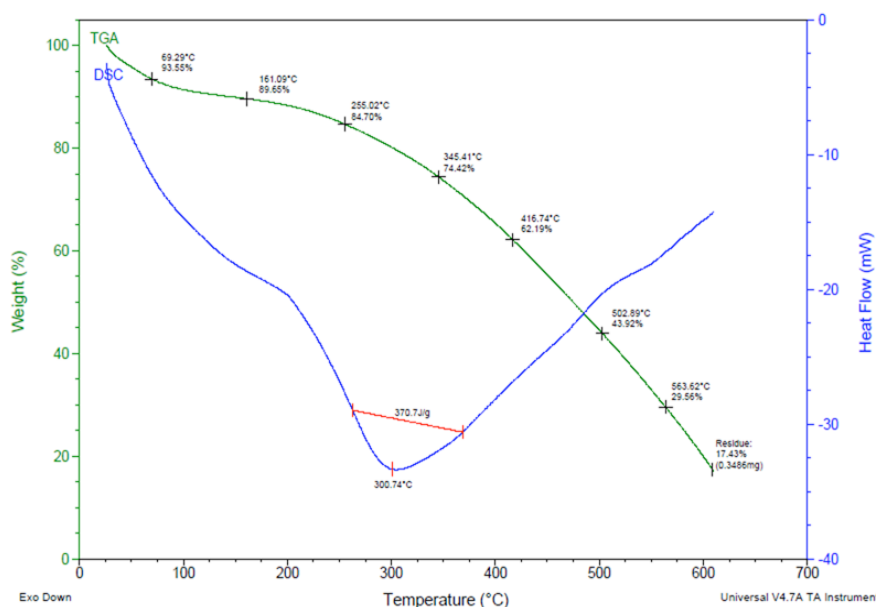


Figure 9: TGA & DSC graph of AA doped PPy.

of dopants from the vicinity of polymer chain. The DSC graph of acrylic acid doped PPy shows one exothermic peak at 573.74 K with the liberation of 370.7 J g^{-1} of energy which reveals the breaking of bonds present in the polymer chain.

The first significant weight loss at 377.27 K [3.31 wt%] in Figure 10 is due to the evaporation of unreacted monomers from the polymer matrix. The second stage weight loss was observed from 467.67 K to 603.61 K [24.23 wt%] is attributed to the degradation of polymer backbone. The third stage weight loss from

603.61 K onwards is due to the loss of dopants from the vicinity of polymer chain. The DSC graph of PAA doped PPy shows one exothermic peak. The peak at the region between 474.45 K and 640.43 K is due to the dissociation of PAA molecules present in vicinity of polymer chain, which was further substantiated by the TGA results by showing the PAA (dopant) degradation at the region of 603.61 K

On comparing the DSC graphs in Figures 9 and 10, the temperature needed for the exothermic reaction in PAA doped PPy is higher (630.43 K) than the AA

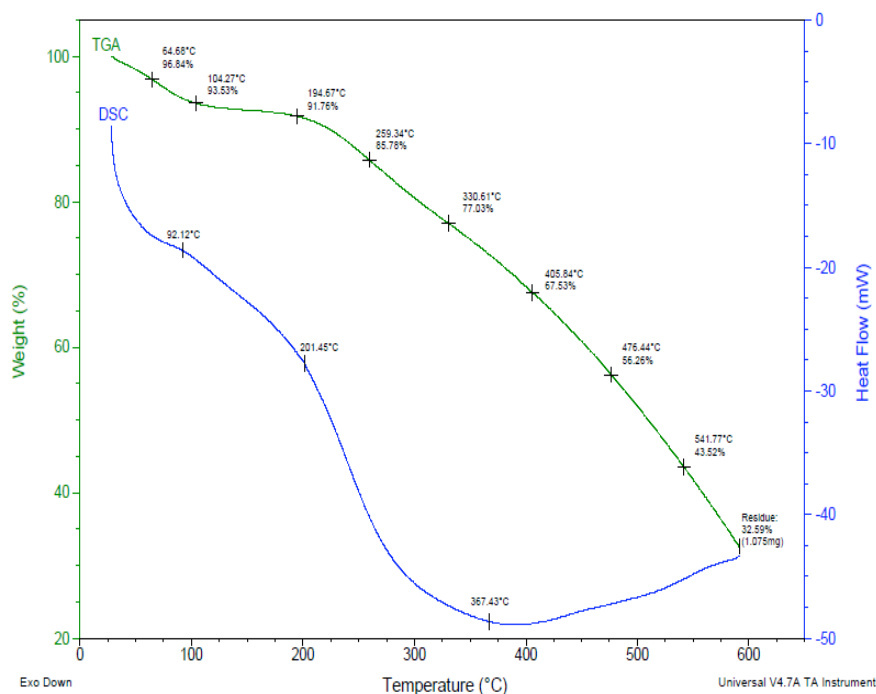


Figure 10: TGA & DSC graph of PAA doped PPy.

doped PPy (573.74 K). which reveals that the energy needed for the dissociation of the polyacrylic acid from the polymer matrix was higher than the energy needed to dissociate the acrylic acid moieties from the polymer matrix. This result shows that the PAA doped PPy was more stable than the AA doped PPy.

3.5. Conductivity Measurements

The electrical conductivities of doped PPy was measured using the four probe method. The room temperature conductivity of PPy is $1.2 \times 10^{-3} \text{ Scm}^{-1}$. Meanwhile, the conductivity of PPy doped with various dopants at room temperature is strongly dependent on the dopant concentration. The increase in conductivity

at high concentration of AA in polymer is due to the incorporation of AA into PPy matrix and serves as a dopant to improve the conductivity of the PPy. This is due to the decrease in size of PPy in presence of AA. Here, the AA plays dual role: it may act as a counter ion to PPy and/or it may act as a capping agent during polymerization. The former has enhanced the conductivity of PPy and the latter controls the morphology of the PPy. The incorporation of the dopant into a PPy can change its electrical properties. The conductivity values of AA doped PPy and PAA doped PPy is given in Table 2. The conductivity of the acrylic acid (AA) doped PPy at 1:1 molar ratio (PPy:AA) is $2.9 \times 10^{-2} \text{ Scm}^{-1}$. The conductivity reaches the maximum at 1:3 molar ratio of PPy:AA to $3.0 \times 10^{-1} \text{ Scm}^{-1}$

Table 2: The Conductivity Values of AA Doped PPy and PAA Doped PPy

Sample	Molar ratio of PPy:dopant	Conductivity (Scm^{-1})
PPy	-	1.2×10^{-3}
PPy:AA	1:1	2.9×10^{-2}
PPy:AA	1:2	6.4×10^{-2}
PPy:AA	1:3	3.0×10^{-1}
PPy:AA	1:4	4.2×10^{-2}
PPy:PAA	1:1	2.1×10^{-2}
PPy:PAA	1:2	5.7×10^{-2}
PPy:PAA	1:3	9.3×10^{-1}
PPy:PAA	1:4	4.3×10^{-2}

Table 3: Solubility Properties of Doped PPy

Sample	Molar ratio of monomer:dopant	Solubility in water
PPy	-	Insoluble
PPy:AA	1:1	Insoluble
	1:2	Insoluble
	1:3	Insoluble
	1:4	Insoluble
PPy:PAA	1:1	Insoluble
	1:2	Slightly soluble
	1:3	Slightly soluble
	1:4	soluble

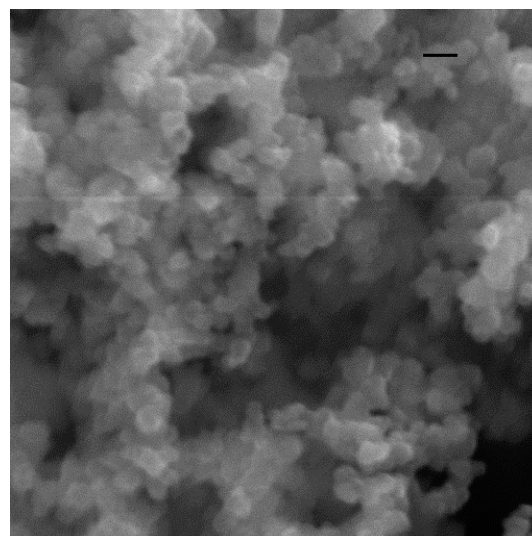
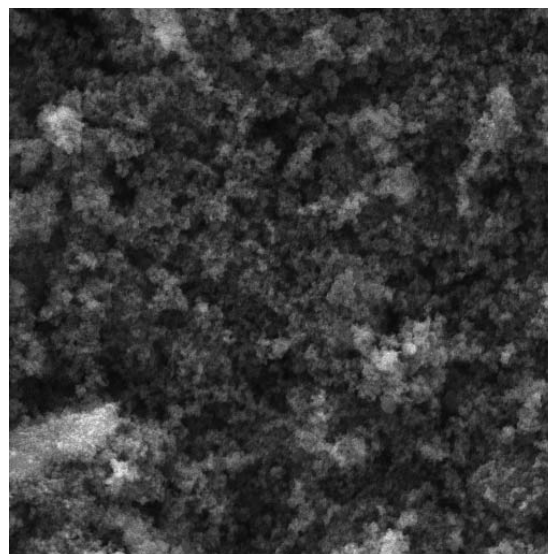
¹ and afterwards, the conductivity get decreased to $4.2 \times 10^{-2} \text{ Scm}^{-1}$ at higher doping level of 1:4 molar ratio of PPy:AA. This decrease in conductivity is due to the presence of high concentration of the dopants (non-conducting species) into the polymer matrix. This shows that the doping process leads to conductivity enhancement only upto certain level. Even the high doping also decreases the conductivity. The same result was observed in the case of the PAA doped PPy. At the 1:1 molar ratio of PPy: PAA, the conductivity is $2.1 \times 10^{-2} \text{ Scm}^{-1}$. The conductivity reaches the maximum of $9.3 \times 10^{-1} \text{ Scm}^{-1}$ at 1:3 molar ratio of PPy: PAA. Again the conductivity decreased to $4.3 \times 10^{-2} \text{ Scm}^{-1}$ at 1:4 molar ratio of PPy: PAA.

3.6. Solubility of Doped PPy in Water

The soluble nature of doped PPy was studied by varying the concentration of the dopants. It was found that the AA doped PPy is insoluble in water. The PAA doped PPy at lower concentration was insoluble in water but at higher concentration (0.25 molar ratio) the PAA doped PPy was soluble in water. Table 3 shows the solubility properties of doped PPy.

3.7. Surface Morphological Studies by Scanning Electron Microscopy (SEM)

SEM images of AA doped PPy and PAA doped PPy was shown in Figures 11 and 12. Figure 11 reveals that the size of the doped PPy get decreases due to the incorporation of AA into PPy spherical particles and serves as a dopant to improve the conductivity of the PPy. Enhancement of conductivity is observed with increase of the AA dopant concentration. This is due to the decrease in size of PPy particles in the presence of AA. Here, the AA plays dual role: it may act as a counter ion to PPy and/or it may act as surfactant during polymerization.

**Figure 11:** SEM image of acrylic acid doped PPy.**Figure 12:** SEM image of polyacrylic acid doped PPy.

The former has enhanced the conductivity of PPy and the latter controls the morphology of the PPy. The

incorporation of the dopant into PPy particles can change its electrical properties. Figure 12 reveals that the size of the doped PPy get decreased due to the incorporation of PAA into PPy spherical particles and serves as a dopant to improve the conductivity of the PPy. Increasing the PAA (dopant) content in PPy improves the conductivity of PPy. This is due to the decrease in size of PPy particles in the presence of PAA. Here also the PAA plays dual role as like the Acrylic acid.

3.8. Electrochemical Impedance Analysis

In the equivalent circuit shown in Figure 13, the resistor R_s represents the resistance of electrolyte. CPE and the R_p represent the constant phase element and resistance of the polymer film. The parallel combination of CPE and R_p (resistor) represents the pseudo-capacitance. The CPE_p element value gives the approximation of capacitive behaviors of the sample. The CPE_p value and its behavior was shown in the Table 4.

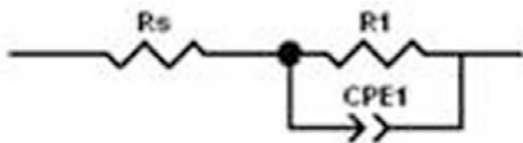


Figure 13: Equivalent circuit.

Table 4: General CPE_p Values with their Capacitive Behavior

CPE_p	Behavior
0	Resistor
1	Pure Capacitor
< 0.75	Super Capacitor

Table 5 shows the capacitance and CPE_p values for the doped PPy. The capacitance can be calculated using the formula given in eq 1, where 'C' is capacitance, 'f' is the frequency and 'Z'' is an imaginary part.

$$C = -1/(2\pi f Z'') \quad (1)$$

The CPE_p value is taken from the equivalent circuit by fitting the circuit with the result obtained for doped PPy. Table 5 shows the CPE_p and capacitance values for the doped PPy

On observing the CPE_p values the PAA doped PPy at higher concentration (1:4) shows the capacitive

behavior which imply that this material has an ability to act as a capacitor.

Table 5: Capacitance and CPE_p Values of PPy Doped with Different Ratios of AA and PAA

Sample	CPE_p	Capacitance (Fcm^{-2})
AA (1:1)	0.36615	2.97×10^{-4}
AA (1:2)	0.42591	1.63×10^{-4}
AA (1:3)	0.56496	2.144×10^{-5}
PAA (1:1)	0.38531	2.81×10^{-4}
PAA (1:2)	0.4932	9.69×10^{-5}
PAA (1:3)	0.74169	4.10×10^{-6}
PAA (1:4)	0.83099	2.11×10^{-5}

Figures 14 and 15 show the Nyquist plot of the AA doped PPy and the PAA doped PPy at different concentrations respectively. The ionic conductivity of the sample (σ) was calculated by the equation $\sigma = L/(RA)$, in which the 'L' is the thickness of the film, 'A' is the surface area of the film and 'R' is the electrical resistance of the material. It was observed that the samples with higher conductivity ($3.0 \times 10^{-1} Scm^{-1}$) are those which have the higher concentration of the dopants. The sample with less amount of dopant has the least conductivity ($2.9 \times 10^{-2} Scm^{-1}$). According to Jacob *et al.* [15], the ionic conductivity of a polymer depends on the concentration of the conducting species and their mobility.

A phase shift for a resistor is $\theta = 0$ at all frequencies, E and I are always 'in-phase'. A capacitor behaves such that the current flowing through it precedes potential, and an ideal capacitor, the phase shift is -90° . An inductor behaves such that current lags behind the potential and for an ideal inductor the phase shift is $+90^\circ$. Both capacitors and inductors are out of phase that is, their current and potential are out of phase. In the Figures 14 and 15, there is no phase shift and the impedance value is independent of frequency.

5. CONCLUSIONS

Doped PPy have synthesized using acrylic acid and poly (acrylic acid) as dopant by the in situ doping chemical polymerization method using $FeCl_3$ as oxidant. We compared the solubility and processability of the doped PPy using different dopants and at different doping levels. The FT-IR studies reveal the presence of the dopant which confirms the incorporation of dopants in the polymer. The UV-Vis

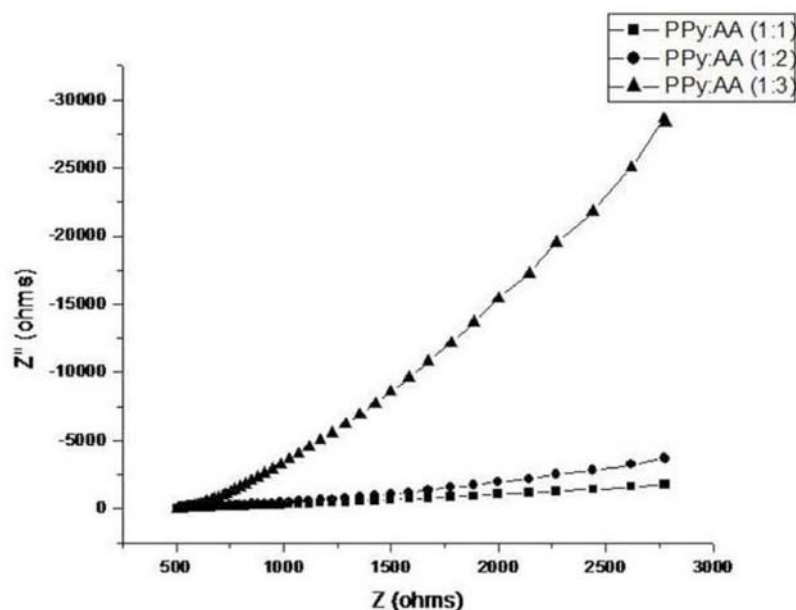


Figure 14: Nyquist plot of acrylic acid doped PPy.

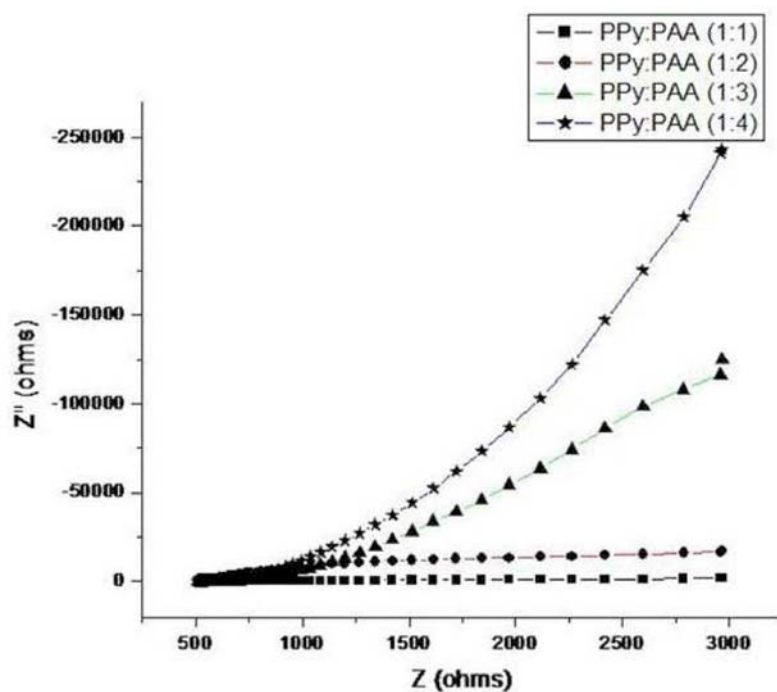


Figure 15: Nyquist plot of polyacrylic acid doped PPy.

study confirms the formation of polaron and bipolaron band in the doped PPy and also reveals the high delocalization. The TGA and DSC analysis reveal that the polymer doped PPy is highly stable than the monomer doped PPy. The polymer doped PPy shows high conductivity than the monomer doped PPy, because the dopant migration in monomer results in loss of charge neutrality but this migration is less in polymer doped PPy. The Electrochemical Impedance Study (EIS) shows that the PAA doped PPy at higher

doping level shows the capacitive behavior. In this study it was found that the PAA doped PPy at higher doping level of 1:4 (PPy: PAA) ratio is soluble in water and 1:3 (PPy: PAA) ratio has high conductivity of $3.0 \times 10^{-1} \text{ Scm}^{-1}$. This reveals that the doping level affects the solubility and conductivity.

ACKNOWLEDGEMENTS

This study was supported by the Technologies and Products for Solar energy utilization through

Networking (TAPSUN) under Council of Scientific Industrial Research, India.

REFERENCES

- [1] Jurewicz K, Delpoux S, Bertagna V, Beguin F, Frackowiak E. Supercapacitors from nanotubes/polypyrrole composites. *Chem Phys Lett* 2001; 347: 363-40. [http://dx.doi.org/10.1016/S0009-2614\(01\)01037-5](http://dx.doi.org/10.1016/S0009-2614(01)01037-5)
- [2] Pernaut JM, Reynolds JR. *J Phys Chem* 2000; 17: 4080. <http://dx.doi.org/10.1021/jp994274o>
- [3] Wu T-M, Lin S-H. Synthesis, characterization and electrical properties of polypyrrole/multiwalled carbon nanotube composites. *J Polym Sci A Polym Chem* 2006; 44: 6449-57. <http://dx.doi.org/10.1002/pola.21724>
- [4] Carrasco PM, Grande HJ, Cortazar M, Alberdi JM, Areizaga J, Pomposo JA. Structure- conductivity relationships in chemical polypyrroles of low, medium and high conductivity. *Synth Met* 2006; 156: 420-25. <http://dx.doi.org/10.1016/j.synthmet.2006.01.005>
- [5] Nalwa HS. *J Mater Sci* 1992; 210: 214.
- [6] Yuan X, Zeng X, Zhang HJ, Ma Z-F, Wang C-Y. Improved performance of proton exchange membrane fuel cells with p-toluenesulfonic acid-doped Co-PPy/C as cathode electrocatalyst. *J Am Chem Soc* 2010; 132: 1754-55. <http://dx.doi.org/10.1021/ja909537g>
- [7] Wu T-M, Chang H-L, Lin Y-W. Synthesis and characterization of conductive polypyrrole with improved conductivity and processability. *Polym Int* 2009; 58: 1065-70. <http://dx.doi.org/10.1002/pi.2634>
- [8] Zdilek CO, Lu JH, Toppare L, Yag Y. *Synth Met* 2004; 140: 69.
- [9] Xue Y, Lu X, Xu Y, Bian X, Kong L, Wang C. *Polym Chem* 2010; 1: 1602.
- [10] Vishnuvardhan TK, Kulkarni VR, Basavaraja C, Raghavendra SG. *Bull Mater Sci* 2006; 1: 29.
- [11] Hogervorst ACR. *Synth Met* 1994; 62: 27. [http://dx.doi.org/10.1016/0379-6779\(94\)90195-3](http://dx.doi.org/10.1016/0379-6779(94)90195-3)
- [12] Athawale AA, Kulkarni MV, Chabukswar VV. *Mater Chem Phys* 2002; 73: 106-10. [http://dx.doi.org/10.1016/S0254-0584\(01\)00338-8](http://dx.doi.org/10.1016/S0254-0584(01)00338-8)
- [13] Tamer U. *Int J Polym Sci* 2009; 14: 259-70.
- [14] Wu T-M, Chang H-L, Lin Y-W. *Polym Int* 2009; 58: 1065-70.
- [15] Jacob M, Prabakaran S, Radhakrishna S. *Solid State Ionic* 1997; 104: 105.

Received on 20-02-2013

Accepted on 27-03-2013

Published on 31-03-2013

DOI: <http://dx.doi.org/10.6000/1929-5995.2013.02.01.8>